

Analysis of two human pre-ribosomal factors, bystin and hTsr1, highlights differences in evolution of ribosome biogenesis between yeast and mammals

Coralie Carron^{1,2}, Marie-Françoise O'Donohue^{1,2}, Valérie Choesmel^{1,2},
Marlène Faubladier^{1,2} and Pierre-Emmanuel Gleizes^{1,2,*}

¹Université de Toulouse, UPS, Laboratoire de Biologie Moléculaire Eucaryote and ²CNRS, LBME,
F-31000 Toulouse, France

Received July 2, 2010; Revised August 3, 2010; Accepted August 4, 2010

ABSTRACT

Recent studies reveal that maturation of the 40S ribosomal subunit precursors in mammals includes an additional step during processing of the internal transcribed spacer 1 (ITS1), when compared with yeast *Saccharomyces cerevisiae*, even though the protein content of the pre-40S particle appears to be the same. Here, we examine by depletion with siRNA treatment the function of human orthologs of two essential yeast pre-ribosomal factors, hEnp1/bystin and hTsr1. Like their yeast orthologs, bystin is required for efficient cleavage of the ITS1 and further processing of this domain within the pre-40S particles, whereas hTsr1 is necessary for the final maturation steps. However, bystin depletion leads to accumulation of an unusual 18S rRNA precursor, revealing a new step in ITS1 processing that potentially involves an exonuclease. In addition, pre-40S particles lacking hTsr1 are partially retained in the nucleus, whereas depletion of Tsr1p in yeast results in strong cytoplasmic accumulation of pre-40S particles. These data indicate that ITS1 processing in human cells may be more complex than currently envisioned and that coordination between maturation and nuclear export of pre-40S particles has evolved differently in yeast and mammalian cells.

INTRODUCTION

During the past 10 years, proteomic and genetic studies have allowed the identification of approximately 190 proteins that play a role in eukaryotic ribosome biogenesis, from the initial nucleolar steps to final processing in the cytoplasm (1–6). These proteins, called pre-ribosomal

factors, display different functions including endo- or exoribonucleases, RNA helicases, chaperones, NTPases or methyl transferases (2,5). They are implicated in ribosome biogenesis but do not form part of mature ribosomes.

Early ribosomal proteins and pre-ribosomal factors assemble co-transcriptionally in the nucleolus with the neo-synthesized pre-ribosomal RNA (pre-rRNA), forming the so-called 90S pre-ribosomal particle (3,7). The large polycistronic rRNA precursor contains the future 18S, 5.8S and 28S mature ribosomal RNAs flanked by external and internal transcribed spacers (ETSs and ITSs), which are progressively removed through endonucleolytic cleavages and exonucleolytic processing (Figure 1A) (8,9). Early processing steps include enzymatic modifications of nucleotides, by 2'-O-ribose methylation or pseudo-uridylation (10,11), together with removal of the 5'- and 3'-ETS and endonucleolytic cleavage of the ITS1 (Figure 1B and C). This latter step splits the 90S particle into pre-40S and pre-60S particles, which then follow two separate processing pathways that involve distinct pre-ribosomal factors (4,12). Both particles are exported from the nucleus and their maturation is completed in the cytoplasm (13–16). Association and dissociation of these numerous pre-ribosomal factors along the maturation pathway renders the composition of pre-ribosomal particles highly dynamic. The exact activity or function of most of the pre-ribosomal factors remains unclear, even when the step at which they are implicated is known.

The list of pre-ribosomal factors composing the pre-40S particles is much shorter than that for the large subunit (3,17–19). Following cleavage of the ITS1, the majority of the factors present in the 90S particle dissociate, although a few remain part of the pre-40S particle, including Enp1p, Dim1p, Rrp12p and Bms1p (3,17). Dim1p, a methyltransferase associated with both the 90S and the pre-40S particles, methylates two adjacent nucleotides in

*To whom correspondence should be addressed. Tel: +33 561 335 927; Fax: +33 561 335 886; Email: gleizes@ibcg.biotooul.fr

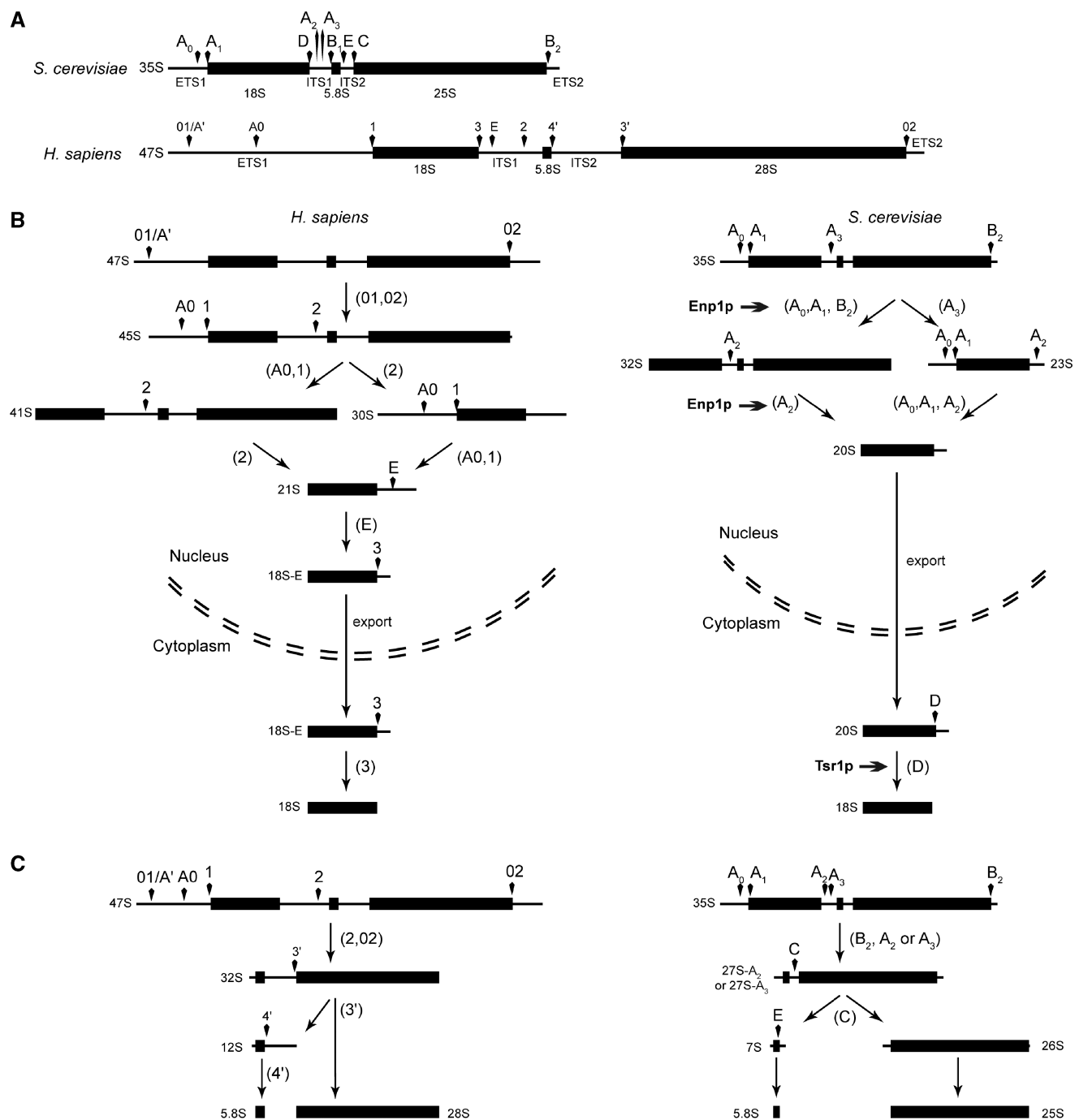


Figure 1. Pre-rRNA processing in HeLa cells. (A) Comparison between the yeast and human large polycistronic rRNA precursor. These two pre-rRNAs have been scale-drawn. (B) 18S rRNA-processing pathways in Human (left panel) and yeast (right panel). Two pathways are presented, according to the kinetics of the ETS1/5'-ETS or ITS1 maturation. The steps at which Enp1p and Tsr1p are involved are indicated. (C) Processing pathways for the large ribosomal subunit RNAs in human (left panel) and yeast (right panel).

the 3'-end of the 18S rRNA (20). Enp1p and Bms1p are known to be implicated in the processing of ETS1 and ITS1 (21–23), but their molecular functions remain unclear. Rrp12p, a HEAT repeat containing protein, is able to interact with nuclear pore complex components and appears to be required for the nuclear export of the pre-40S particle (24). These proteins are joined by other pre-ribosomal factors that assemble specifically with the

pre-40S particle. Hence, Ltv1p in yeast, as well as the kinase hRio2 in human, were proposed as adapters for exportin Crm1p which is required for transport to the cytoplasm (25,26). Hrr25p, a protein kinase, regulates association of the ribosomal protein Rps3p to the pre-40S particle, allowing a structural modification of the pre-40S particle beak, which could be required for passage through the nuclear pore complex (27). The Rio kinases and Tsr1p

are also required for the final cytoplasmic steps, but their molecular function remains to be elucidated (22,28,29). Finally, Nob1p is the endoribonuclease responsible for the cleavage at site D, which matures the 20S pre-rRNA into the 18S rRNA in the cytoplasm (30–33).

Assembly of the pre-ribosomal factors into pre-ribosomes is presumably highly coordinated with pre-rRNA processing and intracellular transport of the particles. Recently, the pre-40S particle composition was characterized in human cells (26). It appears that the pre-ribosomal factors assembled in the pre-40S particle are highly conserved between *Saccharomyces cerevisiae* and human cells. However, ITS1 processing in yeast and mammals is clearly different. After ITS1 cleavage at site A₂ in yeast, elimination of the ITS1 within the pre-40S particles requires a single cytoplasmic cleavage step at the 3'-end of the 18S rRNA (Figure 1B) (13). In contrast, one detects two abundant intermediates in pre-40S particles in mammalian cells, namely the 21S and 18S-E pre-rRNAs. These RNAs correspond to two processing steps, the 21S pre-rRNA being cleaved in the nucleus and the 18S-E species in the cytoplasm (15) (Figure 1B). Therefore, even if the protein content of pre-40S particles is conserved, the pre-ribosomal factors must have evolved to accommodate an increase in complexity of pre-rRNA maturation from yeast to mammals.

To further investigate similarities and differences between yeast and human 40S ribosomal subunit biogenesis, we have studied the role of the human orthologs of two pre-ribosomal factors implicated at two distinct steps of pre-40S particle processing in yeast: Enp1p and Tsr1p. These factors are both essential in yeast. In addition, they are involved at different steps of pre-40S maturation: Enp1p is required for efficient cleavage of the ITS1 in the nucleus (7), whereas Tsr1p is necessary for cleavage at the 3'-end of the 18S rRNA in the cytoplasm (22,28,29). hTsr1, the human ortholog of Tsr1p, was recently found in human pre-40S particles, but its specific role in 40S subunit production is still unclear (26). Bystin/Enp1, the human ortholog of Enp1p, was first identified as a component of a cytoplasmic complex-mediating adhesion of human trophoblast and endometrial epithelial cells *in vitro* (34,35), as well as an essential protein for early embryonic development after implantation of the embryo in mouse and rat (36–38). Recently, it was reported that human bystin is overexpressed in hepatocellular carcinoma (HCC) and is essential for cell growth and tumor development (39). The involvement of bystin in ribosome biogenesis has also been described (38,40). Further analysis of the functions of bystin and hTsr1 in human ribosome biogenesis indicates that these two proteins are indeed functional orthologs of their yeast counterparts, but highlights differences in pre-40S particle biogenesis between yeast and human.

MATERIALS AND METHODS

Plasmids

To construct pEGFP-bystin and pEGFP-hTsr1, bystin and hTsr1 cDNAs were generated by RT-PCR and

cloned into the HindIII and XbaI sites of pEGFP-C3 (Clontech Laboratories, Mountain View, CA, USA), in-frame with the sequence encoding EGFP. EGFP alone was expressed from pEGFP-C3. Transfection of HeLa cells was performed by electro-transformation with 10 µg of plasmidic DNA, as described below for siRNAs.

Cell culture and inhibitor treatments

Human cervical carcinoma HeLa cells were grown in Dulbecco's Modified Eagle Medium (DMEM) containing Glutamax® as a supply of L-glutamine, and supplemented with 10% fetal calf serum (FCS), 1 mM sodium pyruvate, 100 U/ml penicillin and 100 µg/ml streptomycin (Invitrogen, Paisley, UK). Cells were incubated at 37°C in 5% CO₂. RNA polymerase I transcription was selectively inhibited by 50 ng/ml actinomycin D for 2 h.

Knockdown of gene expression with small interfering RNAs

Two or three 21-mer siRNA duplexes were designed and purchased from Eurogentec (Seraing, Belgium) to knockdown expression of human genes encoding bystin (GenBank accession number: NM_004053) and hTsr1 (GenBank accession number: NM_018128), which are two ribosomal factors associated with the small 40S subunit. After washing the cells once in DMEM (without serum and antibiotics), 10 µl of 100 µM siRNA solution were added on ice to 10⁷ HeLa cells in suspension in 200 µl of the same medium. Electro-transformation was performed at 250 V and at 950 µF with a Gene Pulser (Bio-Rad, Hercules, CA, USA), in a cuvette with a 4-mm inter-electrode distance. The cell suspension was then plated on a 200-cm² Petri dish containing 20 ml DMEM supplemented with calf serum and antibiotics. Control samples were electro-transformed with a scramble siRNA (siRNA-negative control duplex; Eurogentec). The efficiency of the downregulation induced by each siRNA was assessed by quantitative reverse transcriptase-PCR, taking GAPDH as an internal control to normalize expression of the target genes. As the most efficient knockdowns were obtained with a mixture of siRNAs *bystin-1* (5'-cugcccaaggcauuu aagadtdt-3') and *bystin-2* (5'-gagguugagacaguugd tdt-3'), and with siRNA *tsr1-1* (5'-cuggaacaguacacuuga dtdt-3'), these conditions were used for the experiments herein described. The siRNA targeting hRPS15 (siRNA *rps15-2*: 5'-UCACCUACAAGCCGUAAA-3') has been described previously (15).

Cell fractionation and RNA extractions

After treatment with siRNAs for 48 h, the cells were successively washed at 4°C with DMEM, PBS and Buffer A (10 mM HEPES, pH 7.9, 1.5 mM MgCl₂, 10 mM KCl). One-tenth of the suspension was kept for total RNA extraction. The cells were then mechanically disrupted with a Dounce homogenizer in Buffer A containing 0.5 mM DTT. After centrifugation at 4°C and at 1000g for 10 min, the supernatant (i.e. cytoplasmic fraction) was frozen. The pellet containing the nuclei was washed with

10 mM Tris-HCl, pH 7.5, 3.3 mM MgCl₂ and 250 mM sucrose. After centrifugation, the nuclei were suspended in a solution containing 10 mM MgCl₂ and 250 mM sucrose, and further purified by centrifugation for 10 min at 500g on a sucrose cushion (0.5 mM MgCl₂, 350 mM sucrose). The pellet was then lysed in 10 volumes of 50 mM Na acetate, pH 5.1, 140 mM NaCl, 0.3% SDS and the nuclear RNAs were extracted twice with phenol. Total and cytoplasmic RNAs were purified with Trizol reagent. After alcohol precipitation, RNA pellets were dissolved in H₂O, quantified using a Nanodrop spectrophotometer (Thermo Fisher Scientific, Waltham, MA, USA) and diluted to 1 mg/ml.

Analysis of ribosomes by sucrose density gradient centrifugation

Forty-eight hours after transfection, HeLa cells were treated with 100 µg/ml cycloheximide (Sigma) for 10 min. The cytoplasmic fractions were prepared on ice as described above, except that cycloheximide was added to all buffers. On each 10–50% (w/w) sucrose gradient, 1 mg proteins was loaded, prepared with a Gradient Master former (BioComp Instruments, Fredericton, NB, Canada). The tubes were centrifuged at 4°C and at 36 000 r.p.m. for 105 min in a SW41 rotor (Optima L100XP ultracentrifuge; Beckman Coulter, Villepinte, France). The gradient fractions were collected at OD_{254 nm} with a Foxy Jr. gradient collector (Teledyne Isco, Lincoln, NE, USA).

Analysis of pre-rRNA species

Pre-rRNA species were analyzed by northern blot. RNAs (3 µg/well for total and nuclear extracts, 6 µg/well for cytoplasmic extracts), mixed with 3 volumes of loading dye (25 mM MOPS, 6% formaldehyde, 1.5% formamide, 0.16 µg/ml BET) were separated on a 1% agarose gel in the presence of MOPS buffer (20 mM MOPS, 6 mM sodium acetate, 7×10^{-2} N NaOH, 0.5 M EDTA pH 8.0) containing 6% formaldehyde, and run in MOPS/formaldehyde buffer (1 × MOPS, 6% formaldehyde) at 140 V. RNAs were then transferred to a Hybond N⁺ nylon membrane (GE Healthcare, Orsay, France). After fixation by UV-crosslinking, the membranes were pre-hybridized for 1 h at 45°C in 6 × SSC, 5 × Denhardt's solution, 0.5% SDS, 0.9 µg/ml tRNA. The ³²P-labeled oligodeoxy-nucleotide probe was then added and incubated overnight at 45°C. The probes used in the present study were 18S (5'-tttacttctcttagatagtcaaggatcgacc-3'), 5'ITS1 (5'-cctcgccctc cgggcctcgtaatgtatc-3'), ITS1-160 (5'-tctccctcccgagtttc gg-3'), ITS1-605 (5'-ttaaacctccgcgcggaaac-3'), ITS1-639 (5'-gacccacggcggacggcgtc-3'), ITS1-721 (5'-ggageggaggat ccgcgtg-3'), ITS1-779 (5'-gtaaacccccacccgacggc-3'), ITS2b (5'-ctgcgagggaaccccccacccgcgea-3'), ITS2d/e (5'-gcccgcggcggacacccgcgcgtc-3') and 28S (5'-cccggttccctt ggctgtgtttcgcttagata-3'). For detection of ITS2, probes ITS2b and ITS2d/e were mixed in equal amounts. After hybridization, the membranes were washed twice for 10 min at room temperature in 2 × SSC, SDS 0.1% and once in 1 × SSC, SDS 0.1%. Labeled RNA signals were acquired with a FLA2000 PhosphorImager.

(Fuji, Stamford, CT, USA) and quantified with ImageGauge software. The 3'RACE analysis was adapted from Kiss and Filipowicz (41). The forward primer used for PCR amplification spanned nucleotides 582–599 in the ITS1: the ITS1-583 primer (5'-ccgcccgtccaggatcaccta-3'). The amplified fragments were subcloned and automatically sequenced.

Detection of fluorescent proteins and fluorescence *in situ* hybridization microscopy

For fluorescence *in situ* hybridization (FISH) experiments, cells grown on glass cover slips were washed twice in PBS and then fixed for 30 min with 4% paraformaldehyde in PBS (EMS, Hartfield, PA, USA). After being rinsed in PBS, cells were permeabilized for 18 h in 70% ethanol at 4°C. After two washes in 2 × SSC containing 10% formamide, hybridization was performed in the dark at 37°C for 5 h in a buffer containing 10% formamide, 2 × SSC, 0.5 mg/ml tRNA, 10% dextran sulfate, 250 µg/ml BSA, 10 mM ribonucleoside vanadyl complexes and 0.5 ng/µl of each probe. Precursors to the 18S rRNA were localized with the 5'-ITS1 probe conjugated to Cy3 or Cy5 (GE Healthcare) on amino-modified deoxythymidine (a probe complementary to the 3'-end of the 18S rRNA and the 5'-end of the ITS1), with the ETS1-b probe (5'-agacgacaacgcctgacacgcacggc-3') conjugated to Cy5 (localized between the 5'-end of the ETS1 and the 01/A' cleavage site), with the ETS1-1399 probe (5'-cgcttagagaaggctttct-3') conjugated to Cy5 (which hybridizes to the 47S pre-rRNA between 01/A' and A0 cleavage sites) or with the 5.8S-ITS2 probe (5'-gcgttgcggcaagcgacgtc-3') conjugated to Cy3 (a probe complementary to the 3'-end of the 5.8S rRNA and the 5'-end of the ITS2). After two washes at 37°C with 2 × SSC containing 10% formamide, the cover slips were rinsed in PBS and DNA was counterstained with 1 µg/ml Hoechst 33342 (Molecular Probes). After 10 min incubation at room temperature, the cover slips were rinsed twice in PBS and mounted in Mowiol 4.88 (Polyscience Inc., Eppelheim, Germany).

For detection of fluorescent proteins after transient transfection, cells grown on glass cover slips were washed twice in PBS and then fixed for 30 min with 4% paraformaldehyde in PBS (EMS). After being washed twice in PBS, DNA was counterstained with Hoechst 33342 for 10 min at room temperature. The cover slips were then rinsed twice in PBS and mounted in Mowiol 4.88.

Observations were made with an inverted IX-81 microscope (Olympus, Rungis, France), equipped with a motorized stage (Märzhäuser, Wetzlar-Steindorf, Germany) and a Coolsnap HQ camera (Photometrics, Tucson, AZ, USA), driven by MetaMorph (Molecular Devices, Downington, PA, USA). Cells were observed using a planapochromat $\times 100$, 1.4 numerical aperture oil immersion objective, mounted on a PIFOC[®] piezo stepper (PI, Karlsruhe, Germany). The light source was a Polychrome V monochromator (Till Photonics GmbH, Gräfelfing, Germany) equipped with a 150 W Xenon source and used with a 15-nm bandwidth. For

multi-labeling experiments, multiband dichroic mirrors (Chroma, Rockingham, VT, USA) were used to avoid pixel shift in the acquisition plane. Specific single-band emission filters were mounted on a motorized wheel (PI). Images were captured with the same exposure times for different samples. The gray levels were scaled within the same limits in order to allow sample comparison. Fluorescence quantification of regions of interest was performed on 12-bit images using MetaMorph software. After background subtraction, the results were expressed as an amount of gray levels/pixel. Fluorescence was quantified in four identical regions of interest in the nucleoplasm and the cytoplasm in at least 24 cells per sample.

RESULTS

Human orthologs of Enp1p and Tsr1p

Bystin presents 55% similarity and 36% identity with yeast Enp1p, whereas hTsrl and Tsr1p share 51% similarity and 30% identity. Similarity between bystin and Enp1p reaches 75% (50% identity) in the C-terminal core domain which defines the specific ‘bystin domain’, whereas their N-termini are more divergent. The bystin domain of Enp1p has a truncated 5' extremity (Figure 2A). Two highly conserved domains are found in hTsrl and Tsr1p: the DUF663 domain, whose function is unknown but which is also found in Bms1; and the AARP2CN domain, which is weakly similar to the GTP-binding domain of elongation factor TU.

When expressed as GFP fusions, both proteins were mainly located in the nucleus and concentrated in the nucleolus, while the cytoplasm was faintly stained (Figure 2B). For bystin, this staining pattern was similar to immunodetection of the endogenous protein (data not shown) and confirmed data from previous reports (26,38,40). After arrest of RNA polymerase I transcription

and segregation of the nucleolar components by actinomycin D treatment (42), both GFP-bystin and GFP-hTsrl were detected in the crescent-shape granular component, consistent with their putative association with pre-ribosomal particles in the nucleolus (Figure 2B).

Bystin and hTsrl are necessary for 40S ribosomal subunit formation

Requirement of bystin or hTsrl for ribosome synthesis was assessed by knocking-down expression of these proteins with siRNAs. In both cases, mRNA levels were reduced by 84–90% (data not shown). Ribosome production after bystin- or hTsrl depletion was analyzed from cytoplasmic fractions prepared in the presence of cycloheximide and separated on sucrose density gradients (Figure 3A). Control cells electro-transformed with a scrambled siRNA displayed a typical profile with peaks corresponding to the 40S and 60S subunits, 80S ribosomal particles and polysomes of increasing lengths. After knocking-down bystin, the levels of free 40S subunits and 80S particles were severely decreased, while 60S subunits accumulated. A similar phenotype was also observed upon depletion of hTsrl, although the decrease in 40S subunits was less pronounced. This imbalance in the levels of 40S and 60S subunits indicates a deficit of 40S production. Consistently, the 18S/28S rRNA ratio was ~30% lower in bystin- or hTsrl-deficient cells than in control cells (see histogram in Figure 3C).

Bystin depletion uncovers an additional step in ITS1 processing

In order to determine the pre-rRNA processing steps of the 40S particle maturation pathway involving bystin and hTsrl, pre-rRNAs were analyzed by northern blot with probes hybridizing to the ITS1 or the ITS2 (Figures 3 and 4). In parallel, the intracellular fate of the pre-ribosomes was monitored by FISH with probes

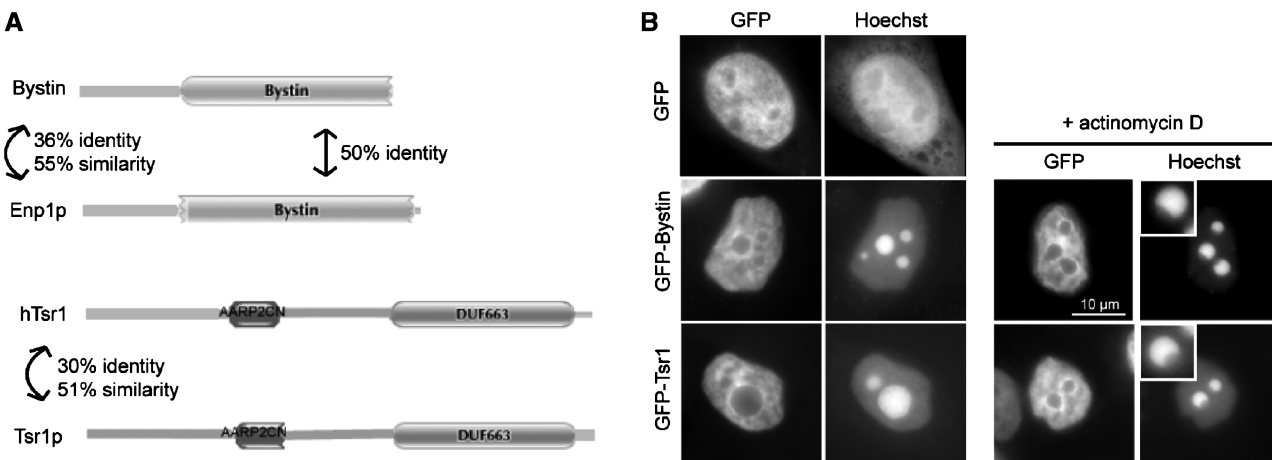


Figure 2. Structural domains and intracellular localization of bystin and hTsrl. (A) A search for specific protein domains was performed with InterProScan. Bystin and Enp1p present a ‘bystin domain’, characteristic of the bystin protein family. hTsrl and Tsr1p have an AARP2CN domain, similar to the GTP-binding domain of the elongation factor TU, and a DUF663 domain of unknown function which is also found in Bms1. (B) Cells transfected with plasmids pGFP, pGFP-bystin or pGFP-hTsrl were observed after chemical fixation and nucleus counterstaining with Hoechst 33342. Treatment with 50 ng/ml actinomycin D for 3 h provokes nucleolar segregation. Boxes show individual nucleoli with a labeled crescent, the characteristic shape of the granular component in segregated nucleoli. Bar = 10 μm.

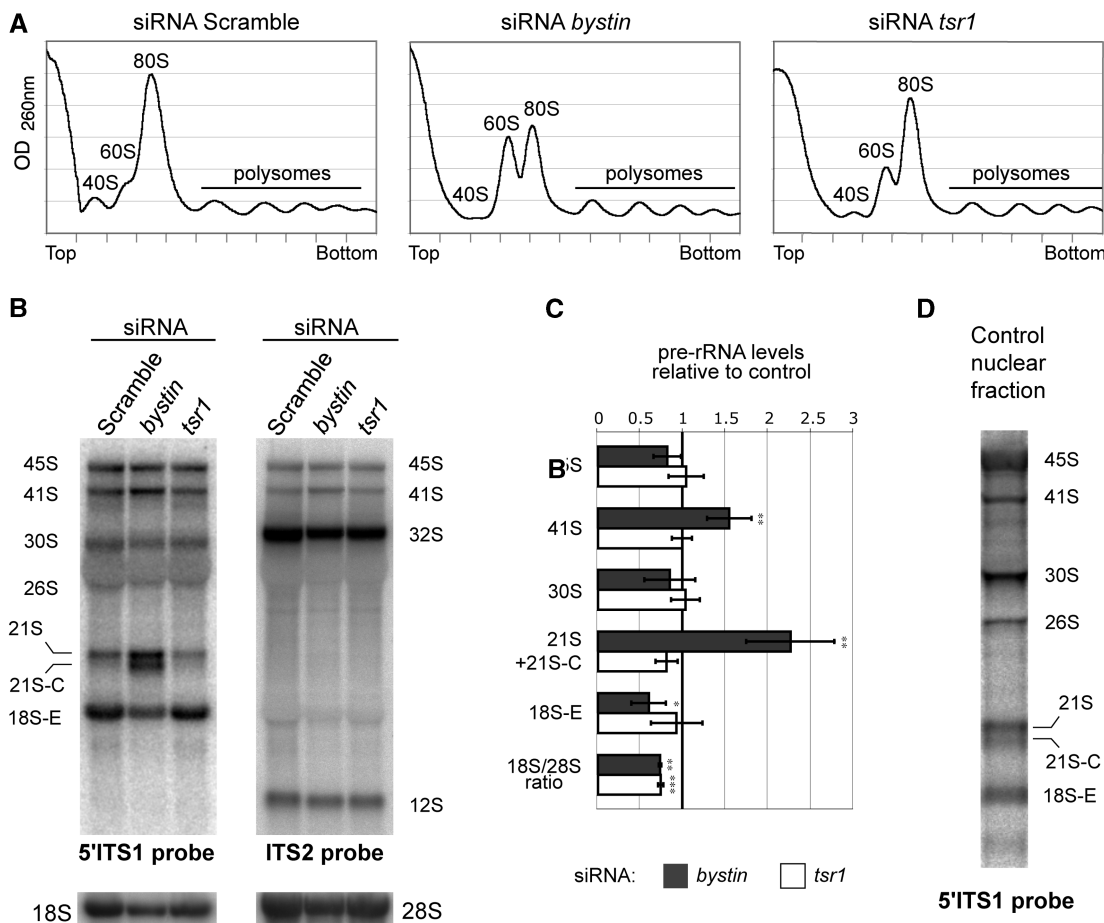


Figure 3. Impact of bystin or hTsrl depletion on ribosome biogenesis. (A) Cytoplasmic fractions, prepared from cycloheximide-treated cells transfected for 48 h either with a scramble siRNA or a siRNA targeting bystin or hTsrl, were separated on sucrose gradients by ultracentrifugation. (B) Identical amounts of RNAs (3 µg) from HeLa cells, extracted 48 h after transfection, were separated on a 1% agarose gel and then transferred to a nylon membrane. The pre-rRNA species were revealed by hybridization with various ³²P-labeled probes (5'ITS1, an equimolar mixture of ITS2b and ITS2d/e, or a mixture of 18S and 28S probes). Pre-rRNAs are described in Figure 1, except the 26S species which extends from site A0 to 2. (C) The labeling of each band was quantified with a phosphorimager and normalized to the amount of 28S RNA measured in the corresponding lane. The means of six different samples in three independent northern blots are presented in the histogram as variation rates relative to control cells. Pair-wise statistical analysis was performed with Student's *t*-test. **P* < 0.05; ***P* < 0.01; ****P* < 0.001. (D) Northern blot analysis with the 5'ITS1 probe shows presence of the 21S-C species in nuclear RNAs from control HeLa cells.

complementary to the 5'-ETS/ETS1, the ITS1 or the ITS2 (Figure 5).

Cells treated with bystin-specific siRNAs over-accumulated 41S and 21S pre-rRNAs, while the amount of 18S-E pre-RNA decreased (Figure 3B and 3C). The build-up of 41S pre-rRNA was also evidenced with the ITS2 probes, while the 32S and 12S large subunit precursors were unaffected compared with control cells. These pre-rRNA patterns indicate delayed cleavage in ITS1 at site 2 and deficient maturation of the 21S pre-rRNA within the pre-40S particles.

In addition, we observed the conspicuous build-up of a shorter form of the 21S pre-rRNA, that we named 21S-C (*court* is the French for short). Such a form was previously described upon depletion of RPS19, and named 20S pre-rRNA (43); however this nomenclature is confusing considering the 20S pre-rRNA in *S. cerevisiae*. Careful examination of total RNAs' northern blot profiles showed the reproducible presence of a shoulder in the

21S peak at this position in control cells, suggesting that the 21S-C is a regular processing intermediate that accumulates upon bystin depletion (data not shown). Indeed, this intermediate could be clearly detected in the nuclear fraction of control cells (Figure 3D).

Additional probes were used to determine the 3'-end of this species by northern blot (Figure 4A). Both the 21S and 21S-C pre-rRNAs were revealed with probes spanning position 170 (ITS1-160) and 615 (ITS1-605) in the ITS1. In contrast, probes hybridizing around nucleotides 650 (ITS1-639) or 730 (ITS1-721) no longer revealed the 21S-C RNA. Considering that at least 15 nt are required for specific hybridization of these oligonucleotidic probes in our experimental conditions, these results indicate that the 3' extremity of the 21S-C pre-rRNA is roughly located between nucleotides 620 and 655 of the ITS1 (Figure 4B). If the 21S-C pre-rRNA resulted from an alternative endonucleolytic cleavage in the ITS1, one would expect the appearance of a complementary cleavage product.

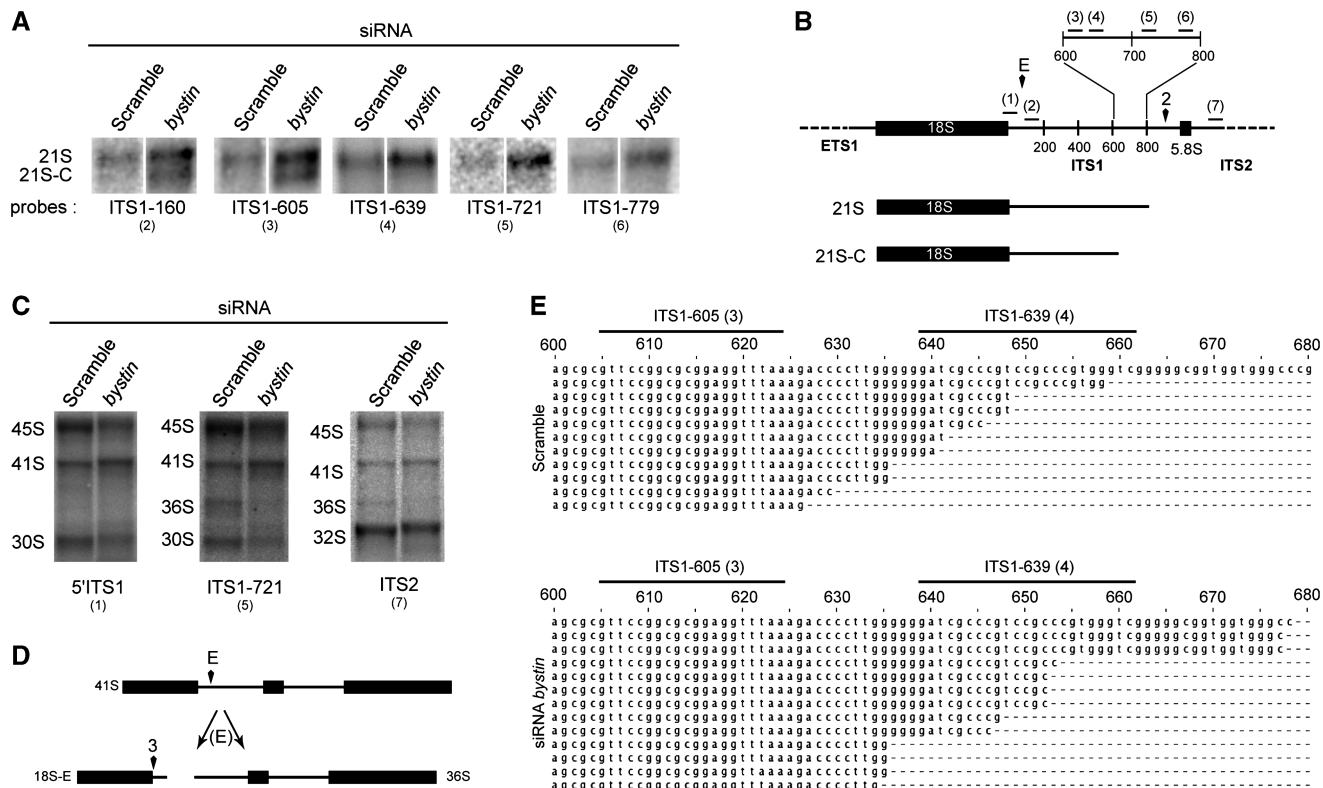


Figure 4. 3' extremity of the 21S-C pre-rRNA. (A) Five specific probes (ITS1-160, ITS1-605, ITS1-640, ITS1-721 and ITS1-779, numbers correspond to nucleotide position within the ITS1) were designed to delineate, by northern blot, the 3'-end of the 21S-C intermediate seen in the absence of bystin. The 21S-C RNA is detected with probe ITS1-605, but not with probes hybridizing downstream in the ITS1 (see position of the probes in D). (B) Schematic representation of the 21S and 21S-C pre-rRNA species and position of the probes. (C) The ITS1-721 and ITS2 probe do not reveal any large species that would be complementary to the 21S-C pre-rRNA, but show disappearance of the 36S pre-rRNA upon bystin deletion. (D) Formation of the 36S pre-rRNA. (E) 3' RACE analysis with primer ITS1-583 shows accumulation of species ending around position 635 and 650 of the ITS1 in bystin-depleted cells. These species are also found in control cells.

However, no pre-rRNA migrating above the 32S RNA was revealed with the ITS1-721 or the ITS2 probes in bystin-depleted cells (Figure 4C). We observed with these probes the disappearance of the 36S pre-rRNA (Figure 4C), a rare precursor that forms upon direct cleavage of early precursors at site E (Figure 4D), which confirms that bystin depletion blocks cleavage at site E.

To further delineate the 3'-end of the 21S-C pre-RNA, we performed 3' RACE experiments with an oligonucleotide spanning nucleotides 582–599 in the ITS1. First, an anchor oligonucleotide was ligated into the 3'-termini of RNAs isolated from whole-cell extracts in order to perform reverse transcription. RNAs with their 3'-end between nucleotide 600 and the anchor were then amplified by PCR, subcloned and sequenced. As shown in Figure 4E, we found several RNAs ending between positions 620 and 650, both in control and in bystin-deficient cells. RNAs from bystin-depleted cells were enriched in species ending around positions 635 and 650. These species were also found in wild-type cells and the heterogeneity of the 3' extremities is consistent with the often-smeary appearance of the band found below the 21S pre-rRNA on northern blots (Figure 3B). This suggests that the 21S pre-rRNA is processed by a 3'-5' exonuclease after cleavage at site 2. In this

hypothesis, the 21S-C could correspond either to the pause or the stalling of this exonuclease, or to the end product of this exonucleolytic processing.

Thus, these data show that bystin participates in efficient cleavage at site 2 and is strictly required for further processing of the 21S pre-rRNA. In addition, they uncover a new processing mechanism in the ITS1.

hTsrl knockdown delays pre-40S particle nuclear export

In contrast to bystin, hTsrl knockdown did not affect the levels of the 18S rRNA precursors when compared with control cells (Figure 3B). Formation of the large subunit rRNAs was not affected either, as seen on the same northern blot revealed with ITS2 probes. However, in the absence of hTsrl, the 18S/28S rRNA ratio strongly decreased, confirming the impact of hTsrl depletion on 40S ribosomal subunit formation observed by sucrose-gradient analyses. These data indicate that hTsrl performs a late function in 18S rRNA maturation and that hTsrl-deficient pre-40S particles are rapidly turned over.

We next analyzed the impact of hTsrl and bystin knockdown on the intracellular fate of pre-ribosomes by FISH, using probes complementary to transcribed spacers 5'-ETS/ETS1, ITS1 and ITS2 (Figure 5). We included in

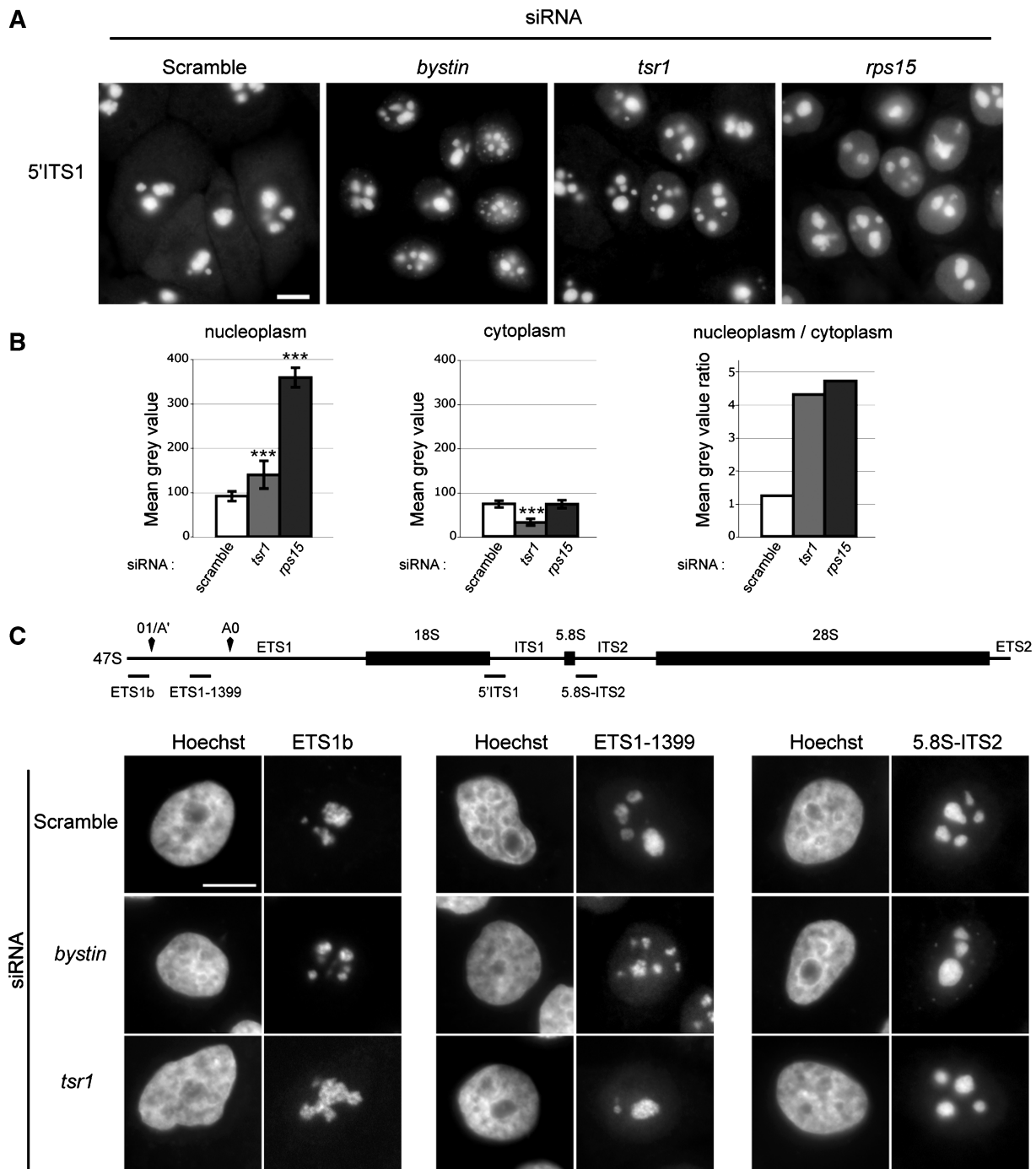


Figure 5. Localization of pre-rRNAs by FISH in bystin- or hTsrl-depleted cells. (A) HeLa cells transfected for 48 h with *bystin*, *tsr1* or *rps15* siRNAs were fixed, hybridized with the 5'ITS1 probe labeled with Cy3 and counterstained with Hoechst 33342. Precursors to the 18S rRNA accumulate in the nucleolus upon bystin depletion, whereas they are found in the whole nucleus in hTsrl and RPS15 depleted cells. Bar = 10 µm. (B) Nucleoplasmic accumulation of pre-40S particles after hTsrl and RPS15 knockdown was measured on a minimum of 30 cells in each condition. Intensity of the FISH labeling (average gray value) was quantified in eight regions of interest, equally dispatched upon the nucleoplasm and the cytoplasm. The graph on the right shows an increase of the labeling ratio between nucleoplasm and cytoplasm in hTsrl and RPS15 depleted cells. In bystin-depleted cells, the presence of bright nucleoplasmic dots made it difficult to reliably quantify fluorescence in the nucleoplasm. ***P < 0.001. (C) HeLa cells transfected for 48 h with *bystin*, *tsr1* or *rps15* siRNAs were hybridized with the 5.8S-ITS2 probe labeled with Cy3, the ETS1b or the ETS1-1399 probe labeled with Cy5. The schematic shows position of the sequences complementary to the probes in the pre-rRNA. Bar = 10 µm.

these experiments cells depleted of RPS15, a ribosomal protein required for nuclear export (15). With the 5'ITS1 probe, cells treated with scrambled siRNAs displayed a strong nucleolar labeling characteristic of the early pre-rRNA species, as well as a cytoplasmic signal indicating the presence in this compartment of 18S-E pre-rRNA, the last precursor to the 18S rRNA (Figure 5A). The labeling level of the nucleoplasm was comparatively weak, attesting rapid trafficking of pre-ribosomal particles through this compartment. In bystin-depleted cells, cytoplasmic labeling decreased whereas nucleoli were conspicuously brighter than in control cells, suggesting accumulation of pre-40S particles in this domain. In addition, nucleoplasmic foci were observed in ~50% of bystin-depleted cells, as previously reported after knockdown of RPS19 or RPS24 (44,45). Using probes complementary to the 5' ETS, no significant differences were detected in bystin-depleted cells compared with control cells (Figure 5C): this suggests that transcription and early pre-rRNA maturation are not affected, which is in accordance with the northern blot results.

In hTsrl-depleted cells, nucleolar labeling was also more intense. In addition, fluorescence was detected in the whole nucleoplasm, similar to that observed in RPS15-depleted cells (Figure 5A), indicating that, in the absence of hTsrl, pre-ribosomal particles are retained in the nucleus. In parallel, the cytoplasm showed almost no fluorescence. This change in pre-40S particle distribution was attested by quantification of the fluorescence signal (Figure 5B). Nucleoplasmic retention in cells depleted of hTsrl was specific of the late pre-40S particles, as it was not observed with the probes complementary to the 5' ETS (Figure 5C).

To strengthen these data, we performed subcellular fractionation followed by northern blot analysis (Figure 6A). Consistent with FISH, the nuclear fraction was enriched in 18S-E pre-rRNA upon hTsrl knockdown (Figure 6B). In bystin-depleted cells, the nuclear fraction was enriched with 41S, 21S and 21S-C pre-rRNAs, whereas the level of 18S-E pre-rRNA decreased, both in the nuclear and in the cytoplasmic fractions. However, the nuclear and cytoplasmic distribution of the 18S-E pre-rRNA still produced in bystin-depleted cells did not change (Figure 6B). These data show that assembly of hTsrl is required for normal trafficking of pre-40S particles from the nucleus to the cytoplasm.

DISCUSSION

The data presented here indicate that bystin and hTsrl are required at distinct steps of the pathway: bystin is necessary for efficient cleavage of the ITS1 at site 2 and for further processing of the pre-rRNA; hTsrl is involved downstream in nuclear export of the pre-40S particles and potentially in final cytoplasmic processing.

Yeast Enp1p is a nuclear protein, concentrated in the nucleolus. This pre-ribosomal factor is required for the earliest cleavages at sites A₀, A₁ and A₂ of the 35S pre-rRNA. Enp1p associates with pre-ribosomes from the 90S particle to the cytoplasmic pre-40S particles (17).

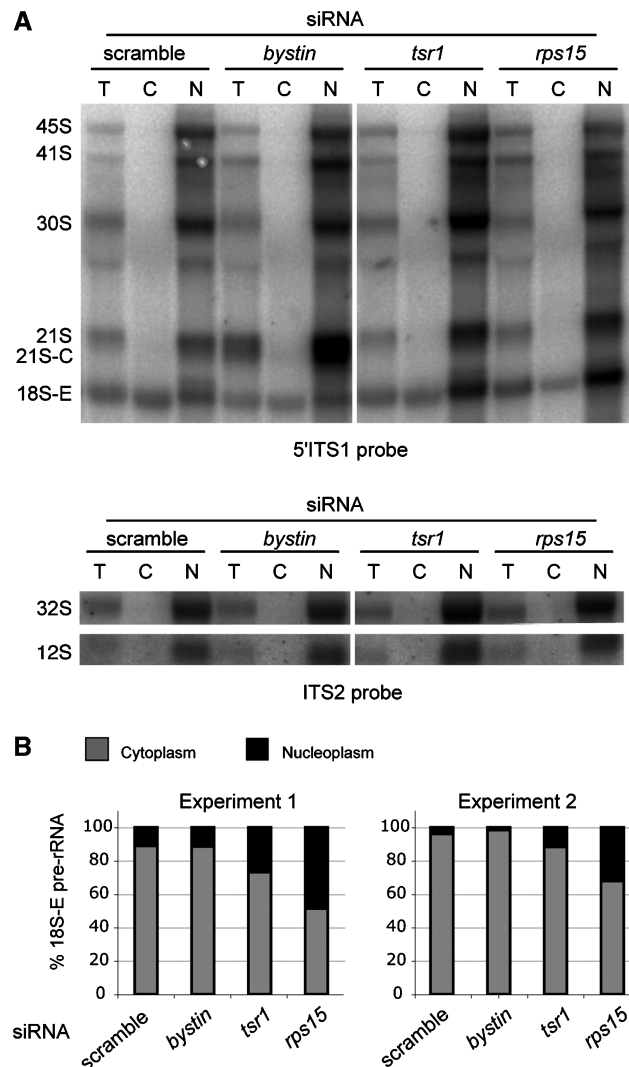


Figure 6. Nuclear retention of pre-40S particle upon depletion of hTsrl. (A) Northern blot analyses of total (T), cytoplasmic (C) or nuclear (N) pre-rRNAs, extracted from cells transfected with bystin, tsrl or rps15 siRNAs for 48 h. RNAs were revealed either with the 5'ITS1 probe or a mixture of ITS2b and ITS2d/e probes. A scramble siRNA was used as a negative control. The cytoplasmic fraction shows no contamination with nuclear pre-rRNAs. (B) The amount of 18S-E pre-rRNA in the cytoplasmic and the nuclear fractions was quantified by phosphorimaging. The histograms show the percentage of 18S-E pre-rRNA found in both fractions in two independent experiments, as calculated from the balance of the whole fractionation procedure.

Depletion of Enp1p affects cleavage of the ETS1 at sites A₀ and A₁ and blocks processing of the ITS1 at site A₂. Alternative cleavage in the ITS1 at site A₃ generates the 23S and 21S aberrant intermediates, whereas 20S pre-rRNA production is blocked (21).

Here, we find that the bystin/hEnp1 human protein is also implicated in pre-40S particle maturation. It is largely located in the nucleus and accumulates in the nucleolus, but it also accompanies the pre-40S particles to the cytosol. Our results confirm previous studies on the intracellular localization of bystin, its presence in pre-40S particles (26,40), and its involvement in ITS1 maturation (38,40). We extend these observations by showing that

depletion of bystin leads to an accumulation of the 41S and 21S pre-rRNAs, which we interpret as a delay in ITS1 cleavage at site 2 and a blockade of ITS1 processing in the pre-40S particles. In addition, a short form of the 21S pre-rRNA accumulates. Given that this species is also detected at low levels in control cells, we think that it could be a short-lived intermediate between the 21S and 18S-E pre-rRNAs. Interestingly, a similar pre-rRNA is observed in human cells upon knockdown of ribosomal protein RPS19 (43), a protein whose depletion in yeast also results in cleavage at site A₃ instead of A₂ and strongly blocks ITS1 maturation in pre-40S particles. The presence of 21S-C pre-rRNA could indicate an alternative endonucleolytic cleavage in the ITS1 preferentially used upon deficient cleavage at site 2. However, we did not detect any cleavage product complementary to the 21S-C pre-rRNA by northern blot. In addition, the heterogeneity of the RNA 3' extremities found in this region by 3'-RACE experiments, together with the fuzzy appearance of this band on northern blots, rather suggest that an exonuclease trims the 21S pre-rRNA after cleavage at site 2. We cannot exclude that this exonuclease is part of a degradation process triggered by the accumulation of 21S pre-rRNA in bystin-depleted cells. However, the presence in control cells of intermediates similar to those found upon bystin knockdown rather supports that this exonucleolytic processing is part of the 21S to 18S-E pre-rRNA conversion and constitutes an additional step in the maturation of the human pre-40S particles.

Accumulation of 21S pre-rRNA as well as disappearance of 36S pre-rRNA upon bystin depletion indicate that bystin is required for cleavage at site E. Processing at site E also requires some RPS proteins, especially RPS18 and RPS19 (46). That RPS19 and bystin depletion yields similar phenotypes may indicate that RPS19 is required for recruitment of bystin to pre-40S particles, as observed in yeast (47). Interestingly, Enp1p and Rps19p in yeast are necessary for ITS1 cleavage at site A₂. This draws an interesting parallel between yeast site A₂ and human site E, although they are, respectively, positioned at 217 nt and ~24 nt from the 18S rRNA 3'-end. Similar to site A₂, cleavage at site E seems to be dependent on processing of the 5'-ETS, as seen upon depletion of some RPS proteins (45,46). Human site 2 in turn is independent of 5'-ETS processing, like site A₃ in yeast.

The role of bystin in ITS1 processing and its association with pre-40S particles indicate that it is a true functional ortholog of yeast Enp1p. However, bystin does not complement a yeast *enp1* null mutant (21). This may be due to the strong divergence of the N-terminal domains of these proteins, which could be required for species-specific functions. In addition, we find no evidence that bystin/hEnp1 is implicated in 5'-ETS maturation, which may be a significant difference in the functions of these proteins.

Yeast Tsrlp localizes to the cytoplasm and the nucleus, including the nucleolus. It associates specifically with pre-40S particles, as indicated by its sole interaction with 20S pre-rRNA and pre-40S-specific factors (27,29). Tsrlp (Twenty-S rRNA) was named due to the large accumulation of 20S pre-rRNA resulting from depletion of this

factor (22,29); when detected by FISH, pre-40S particles are found to pile-up in the cytoplasm (29).

The 40S/60S subunits imbalance detected here on sucrose gradients, confirmed by the reduction of the 18S/28S ratio, argues for a major role of hTsrl function in 40S subunit production. However, unlike in yeast, we observed no major accumulation of pre-rRNAs in the cytoplasm of HeLa cells treated with *tsr1* siRNAs, but instead nucleoplasmic retention of pre-40S particles. This discrepancy may correspond to different coordination between pre-rRNA maturation and nuclear export of pre-40S particles in yeast and mammalian cells. Indeed, production of 18S rRNA requires two pre-rRNA processing steps in human pre-40S particles instead of one in yeast. Our results indicate that hTsrl is not necessary for the first step, i.e. conversion of 21S to 18S-E pre-rRNA. By analogy with yeast Tsrlp, hTsrl may thus be involved in the final cytoplasmic processing step. But prior to this second processing step, assembly of hTsrl is required for efficient nuclear export. Whether hTsrl has a direct role in pre-ribosomal transport to the cytoplasm, for example, as an exportin adaptor, remains to be demonstrated. We found no leucine-rich nuclear export sequence in hTsrl by computer search, unlike recently shown for hRio2 (26). This does not formally exclude the presence of such a sequence, given the weak consensus by which it is defined. The absence in the mammalian orthologs of Mex67p and Mtr2p of a loop critical for the function of these factors in yeast pre-60S particle nuclear export illustrates that pre-ribosomal transport has evolved between yeast and mammals (48). Alternatively, hTsrl may be more indirectly required for correct assembly or folding of the pre-40S particles prior to nuclear export. The fact that 18S-E pre-rRNA does not accumulate in hTsrl-depleted cells suggests that hTsrl-deficient pre-40S particles are very labile and more rapidly degraded in mammalian cells than in yeast.

In conclusion, these data illustrate that, although the pre-40S particle-specific factors have clear functional homologies, maturation and nuclear export of these particles are not governed by strictly similar mechanisms in yeast and human cells. We propose that this is linked to differences in ITS1 processing, which change the timing between the maturation of the particle and its competence for nuclear export. In addition, the potential additional pre-rRNA processing step revealed upon knockdown of bystin or RPS19 indicate that nuclear processing of the ITS1 in mammalian cells may be even more complex than currently envisioned.

ACKNOWLEDGEMENTS

The authors wish to thank Guillaume Stahl, Célia Plisson-Chastang and Milena Preti for scientific discussions, as well as Ulrike Kutay and Sébastien Fribourg for sharing reagents. They are also indebted to Caroline Monod for proofreading the manuscript. C.C. designed and performed most of the experiments, M.-F.O'D. and V.C. and M.F. performed some of the experiments.

P.-E.G. supervised the project. C.C., M.-F.O'D. and P.-E.G. were involved in writing the manuscript.

FUNDING

CNRS, the University of Toulouse and the French National Research Agency (ANR – RIBEUC project); P.E.G. is a fellow of the Institut Universitaire de France; doctoral fellowship from the Ministère de l'Enseignement Supérieur et de la Recherche and from the Association pour la Recherche sur le Cancer (to C.C.). Funding for open access charge: CNRS.

Conflict of interest statement. None declared.

REFERENCES

1. Fatica,A. and Tollervey,D. (2002) Making ribosomes. *Curr. Opin. Cell Biol.*, **14**, 313–318.
2. Fromont-Racine,M., Senger,B., Saveanu,C. and Fasiolo,F. (2003) Ribosome assembly in eukaryotes. *Gene*, **313**, 17–42.
3. Schafer,T., Strauss,D., Petfalski,E., Tollervey,D. and Hurt,E. (2003) The path from nucleolar 90S to cytoplasmic 40S pre-ribosomes. *EMBO J.*, **22**, 1370–1380.
4. Tschochner,H. and Hurt,E. (2003) Pre-ribosomes on the road from the nucleolus to the cytoplasm. *Trends Cell Biol.*, **13**, 255–263.
5. Milkereit,P., Kuhn,H., Gas,N. and Tschochner,H. (2003) The pre-ribosomal network. *Nucleic Acids Res.*, **31**, 799–804.
6. Li,Z., Lee,I., Moradi,E., Hung,N.J., Johnson,A.W. and Marcotte,E.M. (2009) Rational extension of the ribosome biogenesis pathway using network-guided genetics. *PLoS Biol.*, **7**, e1000213.
7. Dragon,F., Gallagher,J.E., Compagnone-Post,P.A., Mitchell,B.M., Porwancher,K.A., Wehner,K.A., Wormsley,S., Settlage,R.E., Shabanowitz,J., Osheim,Y. *et al.* (2002) A large nucleolar U3 ribonucleoprotein required for 18S ribosomal RNA biogenesis. *Nature*, **417**, 967–970.
8. Eichler,D.C. and Craig,N. (1994) Processing of eukaryotic ribosomal RNA. *Prog. Nucleic Acid Res. Mol. Biol.*, **49**, 197–239.
9. Venema,J. and Tollervey,D. (1999) Ribosome synthesis in *Saccharomyces cerevisiae*. *Annu. Rev. Genet.*, **33**, 261–311.
10. Maden,B.E. (1990) The numerous modified nucleotides in eukaryotic ribosomal RNA. *Prog. Nucleic Acid Res. Mol. Biol.*, **39**, 241–303.
11. Kiss,T. (2002) Small nucleolar RNAs: an abundant group of noncoding RNAs with diverse cellular functions. *Cell*, **109**, 145–148.
12. Granneman,S. and Baserga,S.J. (2004) Ribosome biogenesis: of knobs and RNA processing. *Exp. Cell Res.*, **296**, 43–50.
13. Udem,S.A. and Warner,J.R. (1973) The cytoplasmic maturation of a ribosomal precursor ribonucleic acid in yeast. *J. Biol. Chem.*, **248**, 1412–1416.
14. Vanrobays,E., Gleizes,P.E., Bousquet-Antonacci,C., Noaillac-Depeyre,J., Caizergues-Ferrer,M. and Gelugne,J.P. (2001) Processing of 20S pre-rRNA to 18S ribosomal RNA in yeast requires Rrp10p, an essential non-ribosomal cytoplasmic protein. *EMBO J.*, **20**, 4204–4213.
15. Rouquette,J., Choesmel,V. and Gleizes,P.E. (2005) Nuclear export and cytoplasmic processing of precursors to the 40S ribosomal subunits in mammalian cells. *EMBO J.*, **24**, 2862–2872.
16. Thomson,E. and Tollervey,D. (2010) The final step in 5.8S rRNA processing is cytoplasmic in *Saccharomyces cerevisiae*. *Mol. Cell Biol.*, **30**, 976–984.
17. Grandi,P., Rybin,V., Bassler,J., Petfalski,E., Strauss,D., Marzioch,M., Schafer,T., Kuster,B., Tschochner,H., Tollervey,D. *et al.* (2002) 90S pre-ribosomes include the 35S pre-rRNA, the U3 snoRNP, and 40S subunit processing factors but predominantly lack 60S synthesis factors. *Mol. Cell*, **10**, 105–115.
18. Nissan,T.A., Bassler,J., Petfalski,E., Tollervey,D. and Hurt,E. (2002) 60S pre-ribosome formation viewed from assembly in the nucleolus until export to the cytoplasm. *EMBO J.*, **21**, 5539–5547.
19. Saveanu,C., Namane,A., Gleizes,P.E., Lebreton,A., Rousselle,J.C., Noaillac-Depeyre,J., Gas,N., Jacquier,A. and Fromont-Racine,M. (2003) Sequential protein association with nascent 60S ribosomal particles. *Mol. Cell. Biol.*, **23**, 4449–4460.
20. Lafontaine,D., Vandenhoute,J. and Tollervey,D. (1995) The 18S rRNA dimethylase Dim1p is required for pre-ribosomal RNA processing in yeast. *Genes Dev.*, **9**, 2470–2481.
21. Chen,W., Bucaria,J., Band,D.A., Sutton,A. and Sternglanz,R. (2003) Enp1, a yeast protein associated with U3 and U14 snoRNAs, is required for pre-rRNA processing and 40S subunit synthesis. *Nucleic Acids Res.*, **31**, 690–699.
22. Gelperin,D., Horton,L., Beckman,J., Hensold,J. and Lemmon,S.K. (2001) Bms1p, a novel GTP-binding protein, and the related Tsrlp are required for distinct steps of 40S ribosome biogenesis in yeast. *RNA*, **7**, 1268–1283.
23. Wegierski,T., Billy,E., Nasr,F. and Filipowicz,W. (2001) Bms1p, a G-domain-containing protein, associates with Rcl1p and is required for 18S rRNA biogenesis in yeast. *RNA*, **7**, 1254–1267.
24. Oeffinger,M., Dlakic,M. and Tollervey,D. (2004) A pre-ribosome-associated HEAT-repeat protein is required for export of both ribosomal subunits. *Genes Dev.*, **18**, 196–209.
25. Seiser,R.M., Sundberg,A.E., Wollam,B.J., Zobel-Thropp,P., Baldwin,K., Spector,M.D. and Lycan,D.E. (2006) Ltv1 is required for efficient nuclear export of the ribosomal small subunit in *Saccharomyces cerevisiae*. *Genetics*, **174**, 679–691.
26. Zemp,I., Wild,T., O'Donohue,M.F., Wandrey,F., Widmann,B., Gleizes,P.E. and Kutay,U. (2009) Distinct cytoplasmic maturation steps of 40S ribosomal subunit precursors require hRio2. *J. Cell Biol.*, **185**, 1167–1180.
27. Schafer,T., Maco,B., Petfalski,E., Tollervey,D., Bottcher,B., Aebi,U. and Hurt,E. (2006) Hrr25-dependent phosphorylation state regulates organization of the pre-40S subunit. *Nature*, **441**, 651–655.
28. Vanrobays,E., Gelugne,J.P., Gleizes,P.E. and Caizergues-Ferrer,M. (2003) Late cytoplasmic maturation of the small ribosomal subunit requires RIO proteins in *Saccharomyces cerevisiae*. *Mol. Cell Biol.*, **23**, 2083–2095.
29. Leger-Silvestre,I., Milkereit,P., Ferreira-Cerca,S., Saveanu,C., Rousselle,J.C., Choesmel,V., Guinefoleau,C., Gas,N. and Gleizes,P.E. (2004) The ribosomal protein Rps15p is required for nuclear exit of the 40S subunit precursors in yeast. *EMBO J.*, **23**, 2336–2347.
30. Fatica,A., Oeffinger,M., Dlakic,M. and Tollervey,D. (2003) Nob1p is required for cleavage of the 3' end of 18S rRNA. *Mol. Cell Biol.*, **23**, 1798–1807.
31. Fatica,A., Tollervey,D. and Dlakic,M. (2004) PIN domain of Nob1p is required for D-site cleavage in 20S pre-rRNA. *RNA*, **10**, 1698–1701.
32. Lamanna,A.C. and Karbstein,K. (2009) Nob1 binds the single-stranded cleavage site D at the 3'-end of 18S rRNA with its PIN domain. *Proc. Natl Acad. Sci. USA*, **106**, 14259–14264.
33. Pertschy,B., Schneider,C., Gnadig,M., Schafer,T., Tollervey,D. and Hurt,E. (2009) RNA helicase Prp43 and its co-factor Pfal promote 20 to 18 S rRNA processing catalyzed by the endonuclease Nob1. *J. Biol. Chem.*, **284**, 35079–35091.
34. Suzuki,N., Zara,J., Sato,T., Ong,E., Bakhet,N., Oshima,R.G., Watson,K.L. and Fukuda,M.N. (1998) A cytoplasmic protein, bystin, interacts with trophinin, tastin, and cytokeratin and may be involved in trophinin-mediated cell adhesion between trophoblast and endometrial epithelial cells. *Proc. Natl Acad. Sci. USA*, **95**, 5027–5032.
35. Suzuki,N., Nakayama,J., Shih,I.M., Aoki,D., Nozawa,S. and Fukuda,M.N. (1999) Expression of trophinin, tastin, and bystin by trophoblast and endometrial cells in human placenta. *Biol. Reprod.*, **60**, 621–627.
36. Nadano,D., Nakayama,J., Matsuzawa,S., Sato,T.A., Matsuda,T. and Fukuda,M.N. (2002) Human tastin, a proline-rich cytoplasmic protein, associates with the microtubular cytoskeleton. *Biochem. J.*, **364**, 669–677.
37. Aoki,R., Suzuki,N., Paria,B.C., Sugihara,K., Akama,T.O., Raab,G., Miyoshi,M., Nadano,D. and Fukuda,M.N. (2006)

- The BySL gene product, bystin, is essential for survival of mouse embryos. *FEBS Lett.*, **580**, 6062–6068.
38. Adachi,K., Soeta-Saneyoshi,C., Sagara,H. and Iwakura,Y. (2007) Crucial role of BySL in mammalian preimplantation development as an integral factor for 40S ribosome biogenesis. *Mol. Cell Biol.*, **27**, 2202–2214.
39. Wang,H., Xiao,W., Zhou,Q., Chen,Y., Yang,S., Sheng,J., Yin,Y., Fan,J. and Zhou,J. (2009) Bystin-like protein is upregulated in hepatocellular carcinoma and required for nucleologenesis in cancer cell proliferation. *Cell Res.*, **19**, 1150–1164.
40. Miyoshi,M., Okajima,T., Matsuda,T., Fukuda,M.N. and Nadano,D. (2007) Bystin in human cancer cells: intracellular localization and function in ribosome biogenesis. *Biochem. J.*, **404**, 373–381.
41. Kiss,T. and Filipowicz,W. (1993) Small nucleolar RNAs encoded by introns of the human cell cycle regulatory gene RCC1. *EMBO J.*, **12**, 2913–2920.
42. Dousset,T., Wang,C., Verheggen,C., Chen,D., Hernandez-Verdun,D. and Huang,S. (2000) Initiation of nucleolar assembly is independent of RNA polymerase I transcription. *Mol. Biol. Cell*, **11**, 2705–2717.
43. Idol,R.A., Robledo,S., Du,H.Y., Crimmins,D.L., Wilson,D.B., Ladenson,J.H., Bessler,M. and Mason,P.J. (2007) Cells depleted for RPS19, a protein associated with Diamond Blackfan Anemia, show defects in 18S ribosomal RNA synthesis and small ribosomal subunit production. *Blood Cells Mol. Dis.*, **39**, 35–43.
44. Choesmel,V., Bacqueville,D., Rouquette,J., Noaillac-Depeyre,J., Fribourg,S., Cretien,A., Leblanc,T., Tchernia,G., Da Costa,L. and Gleizes,P.E. (2007) Impaired ribosome biogenesis in Diamond-Blackfan anemia. *Blood*, **109**, 1275–1283.
45. Choesmel,V., Fribourg,S., Aguissa-Toure,A.H., Pinaud,N., Legrand,P., Gazda,H.T. and Gleizes,P.E. (2008) Mutation of ribosomal protein RPS24 in Diamond-Blackfan anemia results in a ribosome biogenesis disorder. *Hum. Mol. Genet.*, **17**, 1253–1263.
46. O'Donohue,M.F., Choesmel,V., Faubladier,M., Fichant,G. and Gleizes,P.E. (2010) Functional dichotomy of ribosomal proteins during the synthesis of mammalian ribosomal 40S subunits (in press).
47. Leger-Silvestre,I., Caffrey,J.M., Dawaliby,R., Alvarez-Arias,D.A., Gas,N., Bertolone,S.J., Gleizes,P.E. and Ellis,S.R. (2005) Specific Role for Yeast Homologs of the Diamond Blackfan Anemia-associated Rps19 Protein in Ribosome Synthesis. *J. Biol. Chem.*, **280**, 38177–38185.
48. Yao,W., Roser,D., Kohler,A., Bradatsch,B., Bassler,J. and Hurt,E. (2007) Nuclear export of ribosomal 60S subunits by the general mRNA export receptor Mex67-Mtr2. *Mol. Cell*, **26**, 51–62.